Semiconductor Physics, Quantum Electronics & Optoelectronics, 2026. V. 29, No 2. P. 191-202.

Hetero- and low-dimensional structures

Temperature-dependent charge accumulation and current-voltage characteristics of $Ag_{7-x}(P_xGe_{1-x})S_5I$ superionic heterostructures for solid-state energy devices

V.S. Bilanych[1], A.A. Slyvka[1], S.I. Vorobiov[2], A.I. Pogodin[1], T.O. Malakhovska[1], I.M. Mohylyuk[1], V. Komanicky[2]

[1]*Uzhhorod National University, 46 Pidhirna Street, 88000 Uzhhorod, Ukraine*
[2]*Pavol Jozef Šafárik University, Park Angelinum 9, Košice 04001, Slovakia*
[*]*Corresponding author e-mail: vitaliy.bilanych@uzhnu.edu.ua*

Abstract. The work investigates temperature-dependent charge accumulation and relaxation processes, as well as the current-voltage characteristics of $Ag|Ag_{7-x}(P_xGe_{1-x})S_5I|Se$ heterostructures with different Ge/P ratios. The current-time dependences $I(t)$ were studied in a potentiostatic mode (0.4 V, 600 s) followed by discharge (0 V, 600 s) at 20 °C and 60 °C. It is shown that the relaxation is described by a bi-exponential model with time constants τ_1 and τ_2, corresponding to fast interfacial and slow diffusion processes, respectively. It was established that with increasing temperature, the relaxation times decrease due to the activation of Ag^+ ion transport and the softening of selenium. Arrhenius analysis revealed different activation energies for the fast (~ 0.1…0.3 eV) and slow (~ 0.05…0.15 eV) processes. The current-voltage characteristics exhibit nonlinear and asymmetric behavior with current maxima associated with interfacial polarization and the formation of Ag_2Se. The minimum relaxation times are observed for the composition $Ag_{6.5}P_{0.5}Ge_{0.5}S_5I$.

Keywords: superionic conductors, argyrodite structure, $Ag_{7-x}(P_xGe_{1-x})S_5I$, solid electrolyte heterostructures, charge-discharge processes, interfacial polarization, solid-state electrochemical devices.

https://doi.org/10.15407/spqeo29.02.191
PACS 66.30.Dn, 66.30.H−, 81.05.Je, 81.05.Mh, 82.45.Yz, 84.60.Rb

Manuscript received 04.02.26; revised version received 12.05.26; accepted for publication 10.06.26; published online 23.06.26.

1. Introduction

Silver-based superionic conductors, in particular argyrodite-family materials $Ag|Ag_{7-x}(P_xGe_{1-x})S_5I|Se$, have attracted significant attention due to their high ionic conductivity, structural flexibility, and promising applications in solid-state electrochemical devices [1–8]. These compounds exhibit ionic conductivity values comparable to those of liquid electrolytes, making them attractive candidates for the development of safe and stable energy storage systems [1–4, 8]. The crystal structure of argyrodites is characterized by a partially disordered Ag^+ cation sublattice and a well-developed three-dimensional network of diffusion pathways [5, 6]. The presence of multiple energetically similar sites and low migration barriers results in a "liquid-like" ionic transport behavior in the solid state [2, 5, 6]. Structural disorder plays a key role in ion transport processes by increasing the number of accessible states for ionic hopping and reducing the activation energy of migration [4, 8]. One of the main approaches to tuning the transport properties is heterovalent substitution $Ge^{4+} \rightarrow P^{5+}$, leading to formation of solid solutions $Ag_{7-x}(P_xGe_{1-x})S_5I$ [8–14]. Such substitution modifies the vacancy concentration in the silver sublattice, redistributes Ag^+ ions, and alters the energy landscape for their migration. The highest ionic conductivity values are typically achieved at intermediate compositions, where an optimal balance between the degree of structural disorder and the connectivity of diffusion pathways is realized [8–12].

In addition to the bulk properties of the electrolyte, interfacial processes play a crucial role in the operation of solid-state electrochemical systems [15, 16]. In heterostructures of the type $Ag|Ag_{7-x}(P_xGe_{1-x})S_5I|Se$, charge transport is governed not only by Ag^+ ion diffusion in the electrolyte bulk but also by electrochemical reactions at the electrolyte–cathode interface. The interaction of Ag^+ ions with selenium leads to the formation of the Ag_2Se phase, which exhibits mixed ionic-electronic conductivity and significantly affects the process kinetics, giving rise to nonlinear system behavior [17–21]. Charge accumulation and relaxation processes in Ag|SE|Se heterostructures are multicomponent in nature and involve both fast processes associated with interfacial phenomena and slow processes governed by bulk diffusion and space-charge accumulation [22, 23]. A pronounced asymmetry

© V. Lashkaryov Institute of Semiconductor Physics of the NAS of Ukraine, 2026
© Publisher PH "Akademperiodyka" of the NAS of Ukraine, 2026

between charging and discharging processes is observed, which is attributed to formation and partial decomposition of the interfacial Ag_2Se region [20, 21, 23].

An important task is a deeper understanding of ion transport mechanisms and interfacial interactions in superionic systems, which can be achieved by the investigation of temperature-dependent charge transport processes in $Ag|Ag_{7-x}(P_xGe_{1-x})S_5I|Se$ heterostructures.

The aim of this work is to establish the regularities of temperature-dependent charge accumulation and relaxation processes, as well as current-voltage (*I–V*) characteristics in $Ag|Ag_{7-x}(P_xGe_{1-x})S_5I|Se$ superionic heterostructures, based on the analysis of current-time dependences *I*(*t*). Particular attention is paid to the role of chemical composition (Ge ↔ P substitution), Ag^+ ion transport mechanisms, interfacial polarization, and phase transformations (formation and decomposition of Ag_2Se), as well as to establishing correlations between process kinetics, *I–V* characteristics, and temperature.

2. Results and discussion

In this work, superionic ceramic materials of $Ag_{7-x}(P_xGe_{1-x})S_5I$ system with different Ge/P ratios were used as the solid electrolyte basis for the heterostructures. The following compositions were investigated: Ag_6PS_5I, $Ag_{6.25}P_{0.75}Ge_{0.25}S_5I$, $Ag_{6.5}P_{0.5}Ge_{0.5}S_5I$, $Ag_{6.75}P_{0.25}Ge_{0.75}S_5I$, and Ag_7GeS_5I, covering the full range of heterovalent substitution $Ge^{4+} \rightarrow P^{5+}$ ($0 \le x \le 1$) [5–8, 14].

Heterostructures of the type $Ag|Ag_{7-x}(P_xGe_{1-x})S_5I|Se$ were fabricated using superionic electrolyte (SE) $Ag_{7-x}(P_xGe_{1-x})S_5I$ in the form of ceramic disks with the diameter ~10 mm and the thickness ~1 mm. A detailed description of the synthesis procedure, ceramic preparation, and heterostructure fabrication is provided in our previous work [23]. A silver electrode (Ag) was applied to one side of the disk. On the opposite side, a selenium (Se) film with a thickness of approximately 8 μm was deposited by thermal evaporation in vacuum. Subsequently, a thin gold layer was deposited onto the selenium surface to serve as a current-collecting contact. Thus, heterostructures of the type Ag|SE|Se were formed, where the silver electrode acts as a source of Ag^+ ions, the superionic electrolyte ensures their transport, and the selenium layer functions as a cathode, at which processes of formation and decomposition of Ag_2Se-type phases occurs.

2.1. Galvanostatic charge-discharge cycling

The processes of charge accumulation and relaxation in $Ag|Ag_{7-x}(P_xGe_{1-x})S_5I|Se$ heterostructures were studied using potentiostatic cycling with recording of current-time dependences *I*(*t*). The experimental procedure involved the sequential application of a voltage $U = 0.4$ V for 600 s (charging mode), followed by reducing the voltage to $U = 0$ V for 600 s (discharging mode). These cycles were repeated for 5 cycles, allowing analysis of the evolution of current responses during the "conditioning" of the electrochemical cell at each temperature. Measurements were carried out at two temperatures: 20 °C and 60 °C.

The *I*(*t*) dependences exhibit a characteristic relaxation behavior for all investigated compositions (Fig. 1). At the moment of voltage application, a sharp current spike is observed, caused by the rapid transport of Ag^+ ions and the charging of the electric double layer at the electrode-electrolyte interface [4, 24]. Subsequently, the current decreases monotonically over time, demonstrating relaxation behavior. Upon switching to the discharge mode ($U = 0$ V), the current changes sign and becomes negative. At the initial moment of discharge, a current spike of opposite polarity is also observed, followed by a gradual decrease in its magnitude over time. This form of *I*(*t*) reflects the reverse motion of Ag^+ ions and the discharge of accumulated space-charge and interfacial charge [23].

At the moment of voltage application (the beginning of charging), a current spike (not shown) is observed, reaching its maximum value. This spike is caused by the rapid transport of Ag^+ ions and the initial charging of the electric double layers at the electrode-electrolyte interfaces. Subsequently, the current decreases monotonically with time, which is associated with system relaxation, redistribution of ions, and polarization buildup.

Upon switching to the discharge mode ($U = 0$ V), the current changes sign and becomes negative. At the initial moment of discharge, a sharp current spike (in absolute value, not shown) is also observed, followed by its gradual decrease (relaxation). This form of *I*(*t*) reflects the reverse motion of Ag^+ ions and the discharge of accumulated space-charge and interfacial charge. All samples exhibit common features: the presence of initial peak current, subsequent relaxation, and a change in current sign upon discharge.

The shape of the current curves strongly depends on both the cycle number and the chemical composition of the electrolyte. With increasing cycle number, the following main features are observed: a reduction in the spread of maximum current values from cycle to cycle; improved reproducibility of the curves; stabilization of the relaxation behavior; and changes in the amplitude of the current response. The most significant changes occur between the first and subsequent cycles, which are associated with the formation of the interfacial region and redistribution of Ag^+ ions [23]. In later cycles (3–5), the *I*(*t*) dependences become more stable and closely resemble each other.

For all studied compositions, increasing temperature leads to the following experimental changes in the *I*(*t*) dependences:

– an increase in initial (maximum) current: at higher temperatures, the current at the initial moment increases, resulting in higher current peaks at the beginning of the curves;

– accelerated current relaxation: the current decay occurs more rapidly, manifested by steeper slopes of the *I*(*t*) curves at early times, and a shorter time to reach a quasi-steady state;

– a reduction in the period of the "long tail": at longer times, the current reaches its steady-state value more quickly, especially for Ge-rich compositions;

– enhanced asymmetry between the charge and discharge processes.

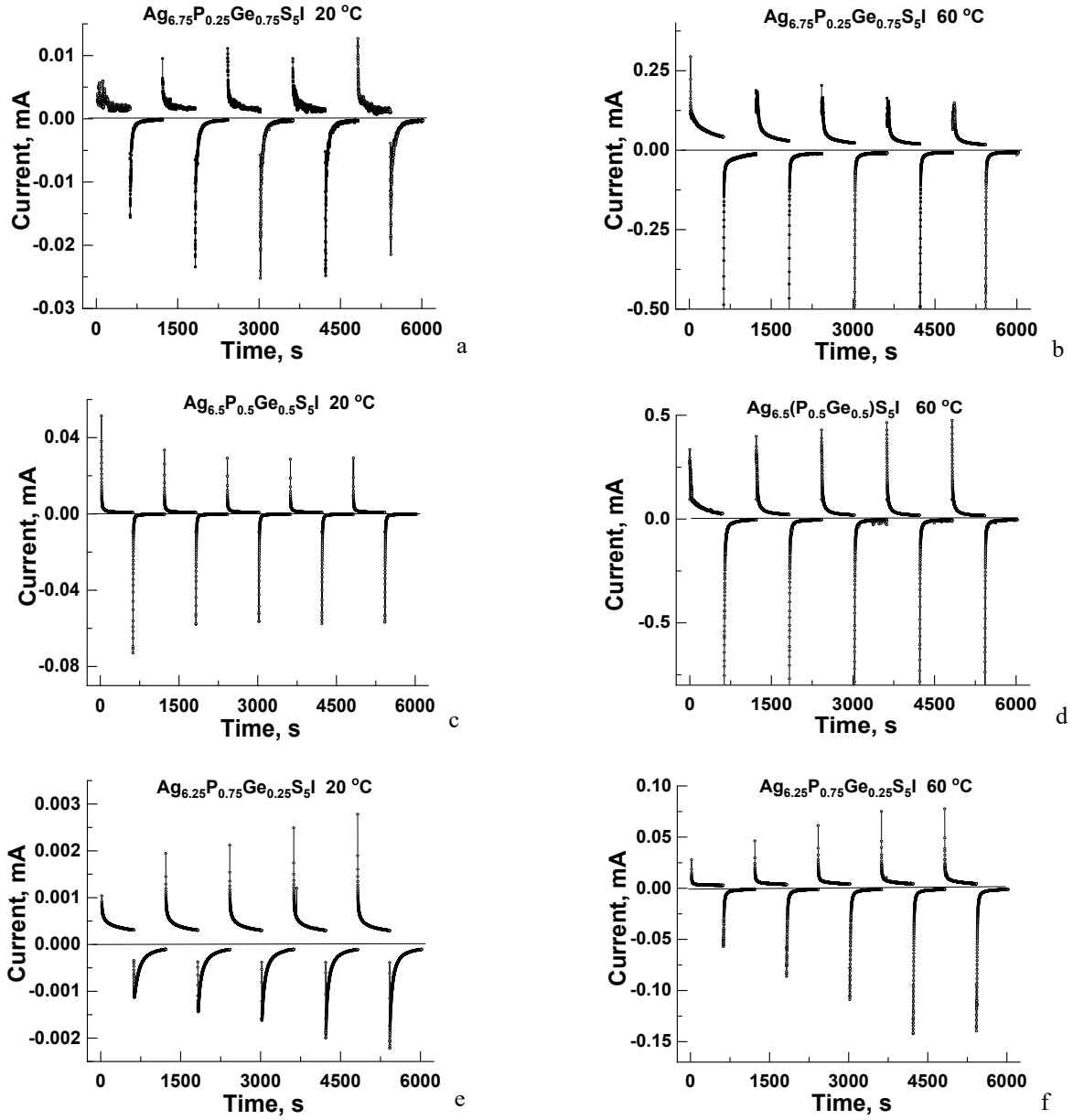

Fig. 1. Current-time dependences $I(t)$ for selected compositions of $Ag_{7-x}(P_xGe_{1-x})S_5I$ at temperatures of 20 °C and 60 °C under a charging voltage of 0.4 V: (a) $Ag_{6.75}P_{0.25}Ge_{0.75}S_5I$, (b) $Ag_{6.5}P_{0.5}Ge_{0.5}S_5I$, (c) $Ag_{6.25}P_{0.75}Ge_{0.25}S_5I$.

At elevated temperatures, the difference between the charging and discharging regions becomes more pronounced: both the amplitude and the shape of the curves change. These effects are attributed to the increased mobility of Ag^+ ions and the reduction of migration energy barriers [2, 25]. In addition, the temperature influence is related to the state of the selenium cathode. Within the temperature range of 50 °C to 80 °C, selenium is in a highly elastic state, which improves interfacial contact and facilitates faster charge transfer processes [26].

These changes are observed for all investigated compositions and retain a common character regardless of chemical composition. For the composition $Ag_{6.75}P_{0.25}Ge_{0.75}S_5I$ (Fig. 1a), the highest initial current value and the fastest current decay are observed. For the composition $Ag_{6.5}P_{0.5}Ge_{0.5}S_5I$ (Fig. 1b), the $I(t)$ dependences exhibit the following features: the presence of a pronounced kink in the curves (change in decay rate); two-stage relaxation with a fast initial decay followed by a slower one; the most noticeable changes in curve shape from cycle to cycle; and intermediate values of current and relaxation times. This composition shows the most distinct separation of time scales, which may be associated with a significant modification of the energy landscape for Ag^+ ion migration [25, 27]. For the composition $Ag_{6.25}P_{0.75}Ge_{0.25}S_5I$ (Fig. 1c), lower initial current values, slower current decay, a pronounced "long tail" of relaxation, and a smoother temporal evolution of the current are observed. The $I(t)$ curves demonstrate more extended relaxation with time.

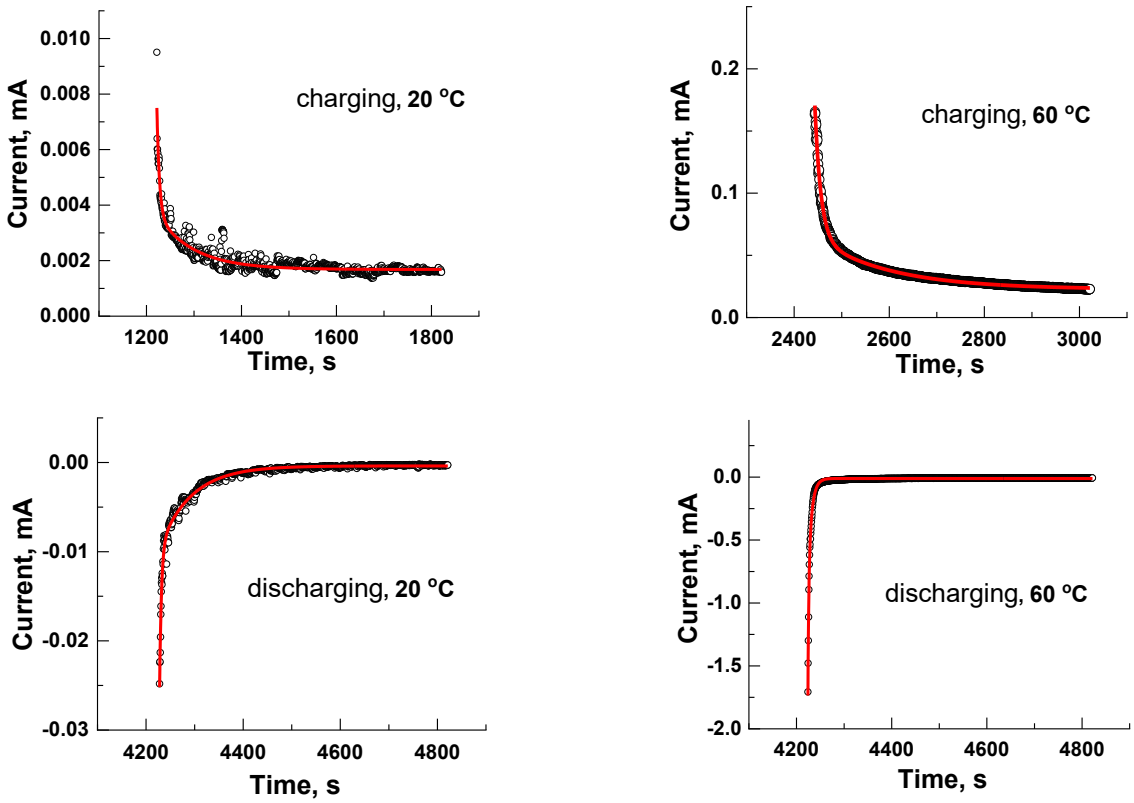

Fig. 2. Current-time dependences $I(t)$ during charging and discharging of the $Ag_{6.75}P_{0.25}Ge_{0.75}S_5I$ heterostructure (fifth cycle) at temperatures of 20 °C and 60 °C, along with the fitting results (red line) obtained using a bi-exponential model.

For a quantitative analysis of the relaxation processes, the experimental $I(t)$ curves obtained during charging and discharging of $Ag|Ag_{7-x}(P_xGe_{1-x})S_5I|Se$ heterostructures were fitted using an exponential function. The fitting results show that the $I(t)$ curves can be well described by a bi-exponential model.

$$I(t) = I_0 + A_1 e^{-\frac{t}{\tau_1}} + A_2 e^{-\frac{t}{\tau_2}},$$

where I_0 is the asymptotic current value at $t \to \infty$; A_1 and A_2 are the amplitudes of the corresponding relaxation processes; and τ_1, τ_2 are the characteristic relaxation times.

The use of a bi-exponential model is justified by the fact that the experimental $I(t)$ dependences cannot be adequately described by a single exponential, indicating the presence of multiple relaxation mechanisms [23].

Fig. 2 shows the $I(t)$ dependences during charging and discharging of the $Ag_{6.75}P_{0.25}Ge_{0.75}S_5I$ heterostructure (fifth cycle) at temperatures of 20 °C and 60 °C, along with the results of fitting using the bi-exponential model. For the other compositions, the $I(t)$ dependences exhibit qualitatively similar behavior.

The relaxation times depend on the cycle number. With an increasing number of cycles, the relaxation times tend to stabilize (the values for the 4th and 5th cycles differ only slightly). The relaxation times τ_1 and τ_2 differ significantly, indicating the presence of fast (initial stage) and slow (final stage) relaxation processes.

The first exponential component with relaxation time τ_1 corresponds to fast processes occurring near the interfacial regions, such as charging of the electric double layer and rapid transport of Ag^+ ions in the near-surface region. The second component with relaxation time τ_2 reflects slower processes associated with bulk ion diffusion, redistribution of space charge, and the development of the interfacial region involving the Ag_2Se phase. The presence of two characteristic relaxation times indicates the multicomponent nature of charge transport processes in the studied heterostructures and confirms that both interfacial and bulk mechanisms make significant contributions. The relative contribution of each component is determined by the amplitudes A_1 and A_2, which also depend on temperature, composition, and cycle number.

Table 1 presents the relaxation times τ_1 and τ_2 for charging and discharging, averaged over the last three cycles. The experimental data indicate the presence of at least two characteristic charge transport mechanisms in $Ag|Ag_{7-x}(P_xGe_{1-x})S_5I|Se$ heterostructures with different time scales. The fast component (τ_1) is associated with processes occurring near the interfacial boundaries, including charging of the electric double layer, redistribution of Ag^+ ions in the near-surface region, and the initial stages of electrochemical interaction with the selenium cathode. The slow component (τ_2) reflects processes occurring in the bulk of the electrolyte and in the interfacial region, including diffusion of Ag^+ ions in

Table 1. Averaged relaxation times τ_1 and τ_2 for charging and discharging processes.

Composition	T, °C	Process	τ_1, s	τ_2, s
$Ag_{6.25}P_{0.75}Ge_{0.25}S_5I$	20	charging	6.24	156.8
$Ag_{6.25}P_{0.75}Ge_{0.25}S_5I$	20	discharging	8.31	73.3
$Ag_{6.25}P_{0.75}Ge_{0.25}S_5I$	60	charging	16.17	174.1
$Ag_{6.25}P_{0.75}Ge_{0.25}S_5I$	60	discharging	3.34	27.1
$Ag_{6.5}P_{0.5}Ge_{0.5}S_5I$	20	charging	1.40	39.9
$Ag_{6.5}P_{0.5}Ge_{0.5}S_5I$	20	discharging	5.57	29.3
$Ag_{6.5}P_{0.5}Ge_{0.5}S_5I$	60	charging	8.00	86.8
$Ag_{6.5}P_{0.5}Ge_{0.5}S_5I$	60	discharging	6.34	76.5
$Ag_{6.75}P_{0.25}Ge_{0.75}S_5I$	20	charging	2.74	112.6
$Ag_{6.75}P_{0.25}Ge_{0.75}S_5I$	20	discharging	32.6	150.5
$Ag_{6.75}P_{0.25}Ge_{0.75}S_5I$	60	charging	1.72	77.0
$Ag_{6.75}P_{0.25}Ge_{0.75}S_5I$	60	discharging	14.9	242.5

the interfacial region, including diffusion of Ag^+ ions in the superionic matrix, accumulation of space charge, as well as growth and restructuring of the interfacial Ag_2Se phase. The observed shape of the $I(t)$ dependences results from the superposition of interfacial and bulk processes.

Significant differences between the first and subsequent cycles indicate a non-stationary nature of the initial state of the system. The first cycle reflects the formation stage of the heterostructure, including the establishment of an effective electrical contact, redistribution of Ag^+ ions, and formation of the interfacial region at the SE|Se boundary. In subsequent cycles, the system transitions to a quasi-stationary state characterized by reproducible $I(t)$ dependences. This is confirmed by the stabilization of the relaxation times τ_1 and τ_2.

The $I(t)$ dependences change with variation in the composition of $Ag_{7-x}(P_xGe_{1-x})S_5I$, reflecting modifications in the structure of the ionic subsystem and the energy landscape of ion migration. The parameters of the $I(t)$ curves for $Ag|Ag_{7-x}(P_xGe_{1-x})S_5I|Se$ heterostructures characterize Ag^+ mobility, charge transport, and relaxation times. Upon Ge → P substitution, systematic changes are observed in both temporal and amplitude parameters of relaxation. In particular, with increasing phosphorus content: the characteristic relaxation times τ_1 and τ_2 increase, indicating a slowdown of both fast and slow charge transport processes; the contribution of the slow component (τ_2) increases, which is manifested by a more pronounced "long tail" in the $I(t)$ dependences; the amplitudes of the fast processes (A_1) decrease, indicating a reduced contribution of rapid interfacial responses; the relative role of slow processes (A_2), associated with diffusion and space-charge accumulation, increases.

For Ge-rich compositions, lower values of τ_1 and τ_2 and higher amplitudes of the fast components are observed, reflecting higher Ag^+ ion mobility and more efficient charge transport.

With changing temperature, the parameters of the charge–discharge processes vary significantly. For a quantitative analysis of the temperature dependence of the relaxation processes characterized by τ_1 and τ_2, an approach based on the Arrhenius equation was employed. It was assumed that the characteristic relaxation times follow a thermally activated behavior:

$$\tau = \tau_0 \cdot e^{\frac{U}{kT}},$$

where τ is the relaxation time (τ_1 or τ_2), τ_0 is the pre-exponential factor, U is the activation energy of the relaxation process, k is the Boltzmann constant, and T is the absolute temperature.

Then, the activation energy can be determined using the following expression:

$$U = k\frac{\ln(\tau_1/\tau_2)}{(1/T_1)-(1/T_2)}.$$

The numerical values of the activation energies and pre-exponential factors are presented in Table 2.

Table 2. Activation energy U_a and pre-exponential factor τ_0.

Composition	Process	Component	U_a, eV	τ_0, s
$Ag_{6.25}P_{0.75}Ge_{0.25}S_5I$	Charging	Fast (τ_1)	~0.137	$\sim 1.3\cdot10^{-2}$
		Slow (τ_2)	~0.131	~0.63
	Discharging	Fast (τ_1)	~0.217	$\sim 5.7\cdot10^{-3}$
		Slow (τ_2)	~0.059	~14.5
$Ag_{6.5}P_{0.5}Ge_{0.5}S_5I$	Charging	Fast (τ_1)	~0.234	$\sim 1.8\cdot10^{-4}$
		Slow (τ_2)	~0.096	~1.6
	Discharging	Fast (τ_1)	~0.009	~4
		Slow (τ_2)	~0.002	~69
$Ag_{6.75}P_{0.25}Ge_{0.75}S_5I$	Charging	Fast (τ_1)	~0.240	$\sim 3.9\cdot10^{-3}$
		Slow (τ_2)	~0.041	~36.7
	Discharging	Fast (τ_1)	~0.158	$\sim 1.5\cdot10^{-2}$
		Slow (τ_2)	~0.300	$\sim 4.7\cdot10^{-4}$

An increase in temperature leads to an acceleration of relaxation processes, manifested by a decrease in the relaxation times τ_1 and τ_2 and an increase in the maximum current. This is associated with thermal activation, enhanced mobility of Ag^+ ions, reduced migration energy barriers, and intensified interfacial reactions. For the investigated $Ag|Ag_{7-x}(P_xGe_{1-x})S_5I|Se$ heterostructures, the state of the selenium cathode is also important. Within the temperature range of 50 °C to 80 °C, selenium is in a highly elastic state [20], which results in a significant reduction of the structural rigidity of the selenium film and, consequently, improves mechanical contact at the SE|Se interface, facilitates Ag^+ ion diffusion in the near-surface region, and may accelerate the formation and restructuring of the Ag_2Se phase. As a result, the temperature effect manifests not only through classical thermal activation but also through changes in the properties of the interfacial region. The activation energy values differ significantly for the fast (τ_1) and slow (τ_2) processes and depend on the heterostructure composition and the operating mode (charging/discharging). For the fast process (τ_1), the characteristic activation energies lie within ~ 0.1…0.3 eV. Higher U values are observed for Ge-rich compositions, indicating more pronounced barrier effects at the interfacial boundaries. For $Ag_{6.5}P_{6.5}Ge_{0.5}S_5I$ during discharging, the U values are close to zero, suggesting an almost barrier-free relaxation process associated with the release of accumulated charge.

For the slow process, the activation energy is generally lower (~ 0.05…0.15 eV). These values correspond to diffusion-controlled transport of Ag^+ ions in the superionic electrolyte and relaxation of space charge. Increasing phosphorus content leads to a decrease in U, which is associated with enhanced structural disordering and facilitated ion migration.

The difference in activation energy for τ_1 and τ_2 confirms that the relaxation processes have different physical origins. The fast process is mainly governed by interfacial phenomena, including ion transport across the SE|Se boundary and the initial stages of Ag_2Se phase formation. The higher U values reflect the presence of energy barriers at the interface. The relaxation time τ_2 (slow process) is associated with bulk diffusion of Ag^+ ions, redistribution of space charge, and development of the interfacial region. Lower U values correspond to a "softer" diffusion-controlled transport regime. At elevated temperatures of the selenium cathode (50…80 °C), interfacial barriers decrease, which is manifested in a reduction of the activation energy, especially for interfacial processes.

One of the key factors determining the shape of the $I(t)$ dependences is the formation of the Ag_2Se phase at the SE|Se interface. During charging, Ag^+ ions migrate toward selenium, where they are reduced, leading to formation of a conductive interfacial region. During discharging, partial reversibility of these processes occurs, accompanied by relaxation of the accumulated charge. The nonlinearity and asymmetry of the $I(t)$ dependences, as well as the differences between charging and discharging, indicate that these processes are not fully reversible.

Based on the obtained results, three main contributions to the formation of the $I(t)$ dependences can be distinguished: fast interfacial processes (τ_1) (charging of the electric double layer and initial Ag^+ transport); slow diffusion processes (τ_2) (bulk transport and space-charge relaxation); interfacial transformations (formation and evolution of the Ag_2Se phase).

2.2. Current-voltage characteristics of Ag|SE|Se electrochemical cells

The I–V characteristics of $Ag|Ag_{7-x}(P_xGe_{1-x})S_5I|Se$ heterostructures were measured using the potentiostatic linear voltage sweep method [16, 24, 28]. The experiments were carried out in a two-electrode configuration using an Autolab PGSTAT302F potentiostat/galvanostat (Metrohm Autolab B.V.) controlled by Nova software. The design of the measurement cell corresponded to that used in our previous work [23]. The Ag|SE|Se heterostructures were connected to the measurement system *via* current-collecting contacts formed on the Ag anode and the Au-coated selenium cathode. Prior to measurements, the samples were held at desired temperature until thermodynamic equilibrium was reached. Temperature control was performed using a chromel-alumel thermocouple. The I–V characteristics were recorded under a linear variation of the applied voltage $U(t)$ following a triangular waveform. The voltage sweep rate was set programmatically and kept constant during each cycle. The following voltage ranges were used: ±0.5, ±1.0, ±1.5, and ±2.0 V. For each range, five consecutive scanning cycles were performed at a fixed sweep rate of 0.025 V/s. This approach allowed evaluation of reproducibility as well as the influence of cycling on the shape of the I–V curves and current magnitude [23, 29].

Additionally, at room temperature, measurements were carried out within a narrow voltage range (−0.5…+0.5 V) at different sweep rates: 0.001, 0.005, and 0.025 V/s. Variation of the scan rate enabled analysis of charge transport kinetics and evaluation of diffusion and interfacial limitations, since in ionic systems the shape of I–V curves strongly depends on relaxation times and charge carrier mobility [16, 30]. During the measurements, the current I was recorded as a function of the applied voltage U for both forward and reverse scans.

The I–V characteristics of the $Ag|Ag_7GeS_5I|Se$ heterostructure, measured at scan rates of 0.025, 0.005, and 0.001 V/s, demonstrate a pronounced dependence of the curve shape on the rate of change of the external electric field (Fig. 3).

The changes in the numerical values of voltages and currents at the maxima U_1, I_1, and U_2, I_2, as well as the current hysteresis ΔI at $U = 0$, were analyzed. These parameters reflect the kinetics of Ag^+ ion transport, interfacial polarization, and relaxation of accumulated charge, see Fig. 3b [16, 24, 28]. The plots show that with increasing scan rate, the current maxima become more pronounced, and the values of I_1 and I_2 increase. This is because, under rapid voltage variation, the system does not have sufficient time to reach a quasi-stationary state.

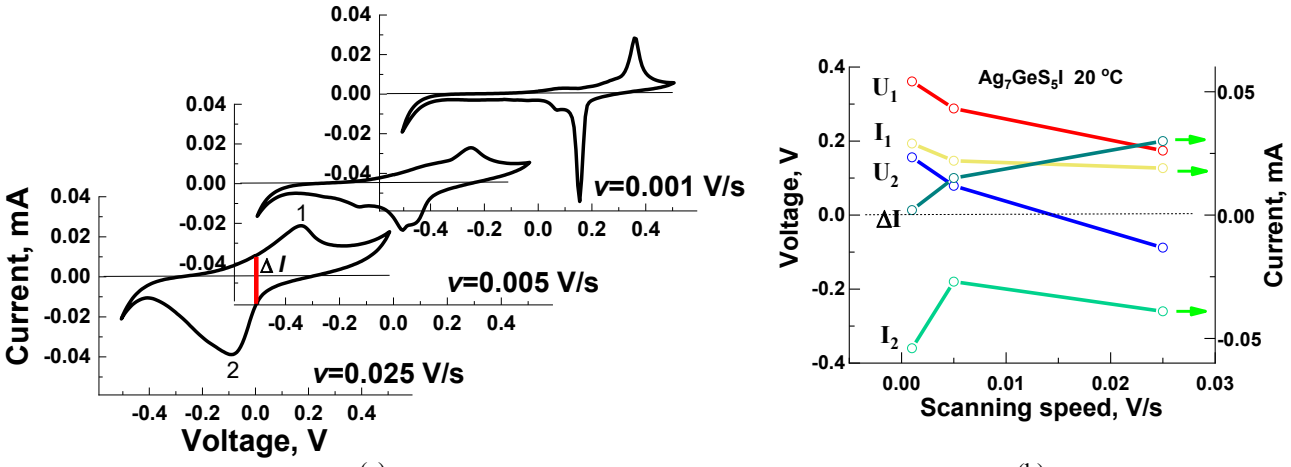

Fig. 3. Dependence of the current-voltage characteristics of the Ag|Ag_7GeS_5I|Se heterostructure on the scan rate (v) at 20 °C (a) and numerical values of voltages and currents at the maxima U_1, I_1, and U_2, I_2, as well as the current hysteresis ΔI at $U = 0$ (b).

Ag^+ ions continue to migrate under the applied field, but their distribution in the electrolyte bulk and near the SE|Se interface lags behind the change in the applied voltage [16, 23]. As a result, the non-equilibrium component of the current increases, which is manifested in the growth of peak magnitudes.

The positions of the maxima U_1 and U_2 also depend on the scan rate. At higher scan rates, the maxima shift toward higher voltages, since a larger overpotential is required to achieve the maximum rate of interfacial reactions. This indicates the presence of kinetic limitations associated with Ag^+ transport through the superionic electrolyte and their interaction with the selenium cathode [28, 29]. When the scan rate decreases from 0.025 to 0.001 V/s, the *I–V* characteristics approach a quasi-stationary regime. The currents decrease, the maxima become smoother, and the hysteresis ΔI at $U = 0$ is reduced. This means that at slower scanning, Ag^+ ions have sufficient time to redistribute, and the SE|Se interfacial region partially relaxes during the measurement [28, 30]. Therefore, the contribution of non-equilibrium polarization decreases. The parameter ΔI, defined as the difference between the forward and reverse currents at $U = 0$, is an important indicator of residual polarization. Its presence indicates that even at zero external voltage, an internal electric field remains in the system, associated with accumulated space charge and a partially formed Ag_2Se-containing interfacial region. An increase in ΔI with increasing scan rate indicates that charge relaxation processes do not have sufficient time to complete within one cycle.

Physically, the observed behavior can be described as a competition between three processes: a fast ionic response of Ag^+ to the external field, a slower diffusion-controlled relaxation in the electrolyte bulk, and interfacial reactions at the SE|Se boundary involving the formation or restructuring of Ag_2Se. At high scan rates, the non-equilibrium and polarization contributions dominate, whereas at low scan rates, the role of diffusion-controlled quasi-stationary transport becomes more significant.

Thus, the dependence of U_1, I_1, U_2, I_2, and ΔI on the scan rate confirms that the *I–V* characteristics of Ag|$Ag_{7-x}(Ge_{1-x}P_x)S_5I$|Se are governed not only by ohmic Ag^+ ion transport but also by slow relaxation and interfacial processes.

The *I–V* characteristics of Ag|$Ag_{7-x}(P_xGe_{1-x})S_5I$|Se heterostructures were also investigated at different temperatures and voltage ranges. The *I–V* curves for the Ag|SE|Se heterostructure based on Ag_7GeS_5I are presented in Fig. 4. For other compositions, the *I–V* characteristics exhibit qualitatively similar behavior.

The obtained *I–V* characteristics exhibit a pronounced nonlinear behavior and differ significantly from ohmic conduction. The *I–V* curves show: asymmetry with respect to zero voltage; the presence of hysteresis between forward and reverse voltage sweeps; current maxima on both anodic and cathodic branches; and a dependence of curve shape on temperature and cycle number. The *I–V* curves form closed loops, the shape of which changes under different measurement conditions.

A comparison of the *I–V* characteristics measured at 20 °C and at an elevated temperature of 60 °C shows that increasing temperature leads to higher absolute current values, enhanced nonlinearity, shifts in the positions of current maxima, and a reduction in the slope of saturation regions. At 60 °C, the *I–V* loops become more "smeared," indicating changes in the kinetics of charge transport processes.

Measurements performed over several consecutive cycles show that the *I–V* parameters evolve from cycle to cycle (Fig. 5). In the initial cycles, more pronounced current maxima, larger hysteresis, and bigger differences between forward and reverse scans are observed. In subsequent cycles, partial stabilization of the curve shape occurs, along with a reduction in parameter dispersion and improved reproducibility of the *I–V* characteristics. This indicates a gradual transition of the system to a quasi-stationary state.

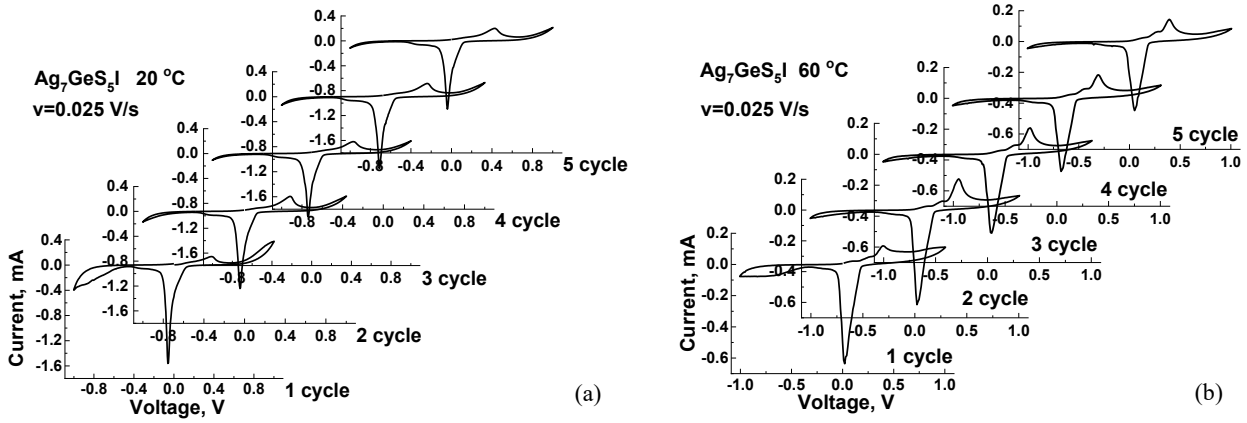

Fig. 4. Current-voltage characteristics of the Ag|SE|Se heterostructure based on Ag_7GeS_5I, measured at temperatures of 20 °C (a) and 60 °C (b), with a scan rate of 0.025 V/s over five consecutive cycles.

Characteristic current maxima are observed in the *I–V* curves, with their position and magnitude depending on temperature and measurement conditions (Fig. 5a). The maxima appear on the anodic branch at positive voltages and on the cathodic branch at negative voltages. With increasing temperature, the maxima on the anodic branch shift toward lower voltages and decrease in amplitude (Figs. 5b, 5c). In contrast, the maxima on the cathodic branch also shift toward lower voltages but increase in amplitude (Figs. 5e, 5f). The presence of these maxima indicates the existence of charge transport limitations and a transition to a regime where the current is governed not only by the applied voltage but also by internal processes within the heterostructure.

All investigated dependences exhibit hysteresis, manifested as a difference in current at the same voltage for forward and reverse sweeps. The hysteresis magnitude ΔI is largest in the initial cycles, decreases with cycling, and depends on temperature. With increasing temperature, the polarization current ΔI decreases, indicating the presence of residual polarization and non-equilibrium processes in the system.

The obtained *I–V* characteristics of $Ag|Ag_{7-x}(P_xGe_{1-x})S_5I|Se$ heterostructures exhibit pronounced nonlinearity and asymmetry, indicating the complex nature of charge transport. In contrast to ohmic behavior, the current is determined not only by the conductivity of the solid electrolyte but also by interfacial and non-equilibrium processes [2, 16, 28]. The asymmetry of the *I–V* curves with respect to zero voltage suggests different transport mechanisms under positive and negative polarization. This is related to the fact that the processes occurring at the SE|Se interface are directional and depend on the direction of Ag^+ ion migration [23, 28].

The presence of maxima on both anodic and cathodic branches is one of the key features of the studied systems. These maxima reflect the transition from a regime of accelerated charge transport to a transport-limited regime governed by internal processes [16, 24]. At the initial stage, as the voltage increases, the current rises due to enhanced Ag^+ ion migration and activation of interfacial processes. The attainment of a current maximum is associated with the accumulation of space charge, formation of the interfacial region, and a reduction in the efficiency of further charge transport. Beyond the maximum, the current either saturates or decreases, indicating a transition to a transport-limited regime [24, 30].

A crucial role in shaping the *I–V* characteristics is played by the interfacial region at the SE|Se boundary, associated with the formation of the Ag_2Se phase. Under positive bias, Ag^+ ions migrate toward selenium, where they are reduced, leading to the formation of a conductive Ag_2Se phase. Upon polarity reversal, partial reversibility of these processes occurs, accompanied by restructuring of the interfacial region. Thus, the *I–V* characteristics reflect not only ion transport but also the dynamics of formation and evolution of the interfacial structure [26, 28].

The presence of hysteresis in the *I–V* curves indicates the non-equilibrium nature of the processes in the system. Hysteresis arises from space-charge accumulation, finite relaxation times of Ag^+ ions, and the inertia of interfacial processes. The parameter ΔI (at $U = 0$) reflects residual polarization of the system. Its presence indicates that even in the absence of an external field, the system remains partially polarized. The magnitude of hysteresis is governed by the relaxation times τ_1 and τ_2: the larger the τ values, the more pronounced the non-equilibrium effects [23, 30].

The significant influence of temperature on the shape of the *I–V* characteristics is due to increased Ag^+ ion mobility, reduced energy barriers, and accelerated interfacial processes at elevated temperatures [2, 16]. This leads to higher currents, smoothing of maxima, and a reduction in hysteresis. An additional factor is the change in the state of selenium with increasing temperature. Within the range 50 °C…80 °C, selenium is in a highly elastic state, which improves contact at the SE|Se interface, increases the effective interaction area, and facilitates the formation of Ag_2Se.

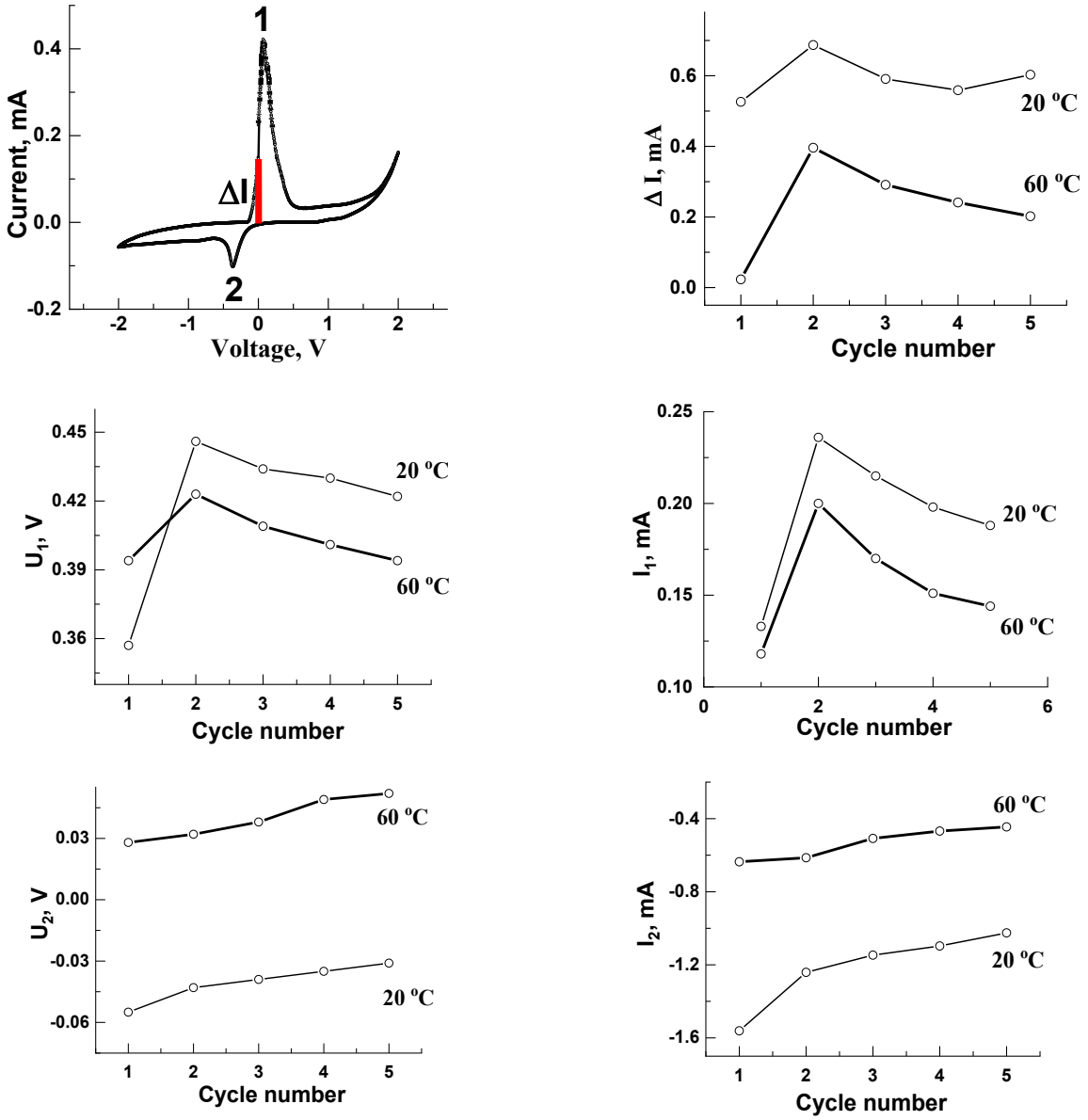

Fig. 5. Change in the parameters of the current-voltage characteristics of the Ag|Ag_7GeS_5I|Se electrochemical cell for $U = \pm 2$ V, scan rate – 0.025 V/s at temperatures of 20 °C and 60 °C during five charge-discharge cycles.

The dependence of the *I–V* characteristics on the scan rate further confirms the non-equilibrium nature of the processes. At high scan rates, the system does not have sufficient time to relax, resulting in increased currents, enhanced hysteresis, and more pronounced maxima. At low scan rates, the system approaches a quasi-stationary state, reducing the contribution of polarization and smoothing the features of the *I–V* curves. This indicates that the characteristic time of the external field variation is comparable to the relaxation times τ_1 and τ_2.

The *I–V* characteristics and *I*(*t*) dependences reflect the same physical processes under different experimental conditions: *I*(*t*) describes temporal relaxation, while *I–V* curves represent the response to a varying electric field. The features of charge-discharge processes observed in both *I*(*t*) and *I–V* characteristics share common mechanisms: fast processes (τ_1) correspond to the initial current rise; slow processes (τ_2) contribute to hysteresis and current maxima; and interfacial processes are responsible for the asymmetry of the *I–V* curves.

The behavior of the *I–V* characteristics can be described as a superposition of three processes: ionic conductivity (Ag^+ transport), diffusion limitations, and interfacial reactions (Ag_2Se formation). Their combined effect leads to the observed nonlinearity, current maxima, hysteresis, and asymmetry. Thus, the *I–V* characteristics of Ag|SE|Se heterostructures reflect a complex interplay of ion transport, interfacial polarization, and the dynamics of Ag_2Se formation, and are a direct manifestation of the non-equilibrium kinetics of the system, closely related to the relaxation processes revealed in *I*(*t*) experiments.

3. Conclusions

This work presents a comprehensive study of temperature-dependent charge accumulation and relaxation processes, as well as current-voltage characteristics of solid-state Ag|$Ag_{7-x}(P_xGe_{1-x})S_5I$|Se heterostructures with varying Ge/P ratios. It was established that the current-time dependences $I(t)$ exhibit a relaxation behavior and are well described by a bi-exponential model, indicating the presence of both fast interfacial and slow bulk diffusion-controlled processes. It was shown that the first charge-discharge cycle corresponds to the formation stage of the heterostructure, whereas in subsequent cycles the system reaches a quasi-stationary state. An increase in temperature leads to accelerated relaxation processes, reduced characteristic times τ_1 and τ_2, and increased current values. This behavior is associated with thermally activated Ag^+ ion transport and changes in the properties of the selenium cathode. Arrhenius analysis confirmed the different nature of fast and slow processes, characterized by distinct activation energies. It was demonstrated that the current-voltage characteristics of the heterostructures exhibit pronounced nonlinearity and asymmetry, with the presence of current maxima and hysteresis. The shape of the *I–V* curves is governed by the competition between ionic transport, diffusion limitations, and interfacial processes at the SE|Se boundary, including the formation and evolution of the Ag_2Se phase. A significant dependence of both $I(t)$ and *I–V* characteristics on chemical composition was observed. The obtained results demonstrate that charge transport in Ag|SE|Se heterostructures is multicomponent and non-equilibrium in nature, governed by the interplay of ionic conductivity, interfacial polarization, and structural factors. The established regularities can be used to develop the next-generation solid-state electro-chemical devices.

Acknowledgements

This work has been supported by the grant of the Ministry of Education and Science of Ukraine under project No. 0126U002381 and the grant of the Slovak Research and Development Agency under the contract APVV-23-0049. S. Vorobiov acknowledges financial support provided under the NextGenerationEU through the Recovery and Resilience Plan for Slovakia under the project No. 09I03-03-V0400179.

References

1. Strauss F., Lin, J., Kondrakov A., Brezesinski T. High-entropy argyrodite lithium superionic conductors. *Matter.* 2023. **6**, No 4. P. 1068–1070. https://doi.org/10.1016/j.matt.2023.03.007.
2. Pogodin A., Filep M., Malakhovska T. *et al*. Influence of recrystallization process on ionic conductivity of $Ag_{6.75}P_{0.25}G_{e0.75}S_5I$ based ceramic materials. *Ceram. Int.* 2023. **49**, No 21. P. 33764–33772. https://doi.org/10.1016/j.ceramint.2023.08.068.
3. Austin M.S., Galinat S.L., Maughan A.E. Complex dynamics in argyrodite solid-state ion conductors. *Chem. Mater.* 2026. **38**, No 7. P. 3038–3058. https://doi.org/10.1021/acs.chemmater.5c02939.
4. Shotwell A.M., Galinat S.L., Maughan A.E. Complex dynamics in argyrodite solid-state ion conductors. *Chem. Mater*. 2026. **38**, No 7. P. 3038–3058. https://doi.org/10.1021/acs.chemmater.5c02939.
5. Li C., Zhang S., Miao X. *et al.* Designing lithium argyrodite solid-state electrolytes for high-performance all-solid-state lithium batteries. *Batteries & Supercaps*. 2021. **5**, No 3. P. 288. https://doi.org/10.1002/batt.202100288.
6. Pogodin A., Filep M., Malakhovska T. *et al*. Recrystallization effect on mechanical parameters and increasing of Ag^+ ionic conductivity in $Ag_7(Si_{1-x}Ge_x)S_5I$ ceramic materials. *Solid State Sci.* 2023. **140**. P. 107203. https://doi.org/10.1016/j.solidstatesciences.2023.107203.
7. Wang H., Ozkan C.S., Zhu H. *et al*. Advances in solid-state batteries: Materials, interfaces, characterizations, and devices. *MRS Bull.* 2023. **48**. P. 1221–1229. https://doi.org/10.1557/s43577-023-00649-7.
8. Yamamoto O. Solid state ionics: a Japan perspective. *Sci. Technol. Adv. Mater.* 2017. 18, No 1. P. 504–527. https://doi.org/10.1080/14686996.2017.1328955.
9. Yu C., Zhao F., Luo J. *et al*. Recent development of lithium argyrodite solid-state electrolytes for solid-state batteries: Synthesis, structure, and properties. *Inorganics*. 2022. **10**. P. 125. https://doi.org/10.3390/inorganics10050125.
10. Bendak A.V., Skubenych K.V., Pogodin A.I. *et al*. Influence of cation substitution on mechanical properties of $(Cu_{1-x}Ag_x)_7GeSe_5I$ mixed crystals and composites on their base. *SPQEO.* 2020. **23**. P. 37–40. https://doi.org/10.15407/spqeo23.01.37.
11. Li C., Wang Z., He Z. *et al*. An advance review of solid-state battery: challenges, progress and prospects. Sustain. *Mater. Technol*. 2021. **29**. P. e00297. https://doi.org/10.1016/j.susmat.2021.e00297.
12. Studenyak I.P., Pogodin A.I., Filep M.J. *et al.* Influence of heterovalent cationic substitution on electrical properties of $Ag_{6+x}(P_{1-x}Ge_x)S_5I$ solid solutions. *J. Alloys Compd.* 2021. **873**. P.159784. https://doi.org/10.1016/j.jallcom.2021.159784.
13. Sau K., Takagi S., Ikeshoji T. *et al.* Unlocking the secrets of ideal fast ion conductors for all-solid-state batteries. *Commun Mater.* 2024. **5**. P. 122. https://doi.org/10.1038/s43246-024-00550-z.
14. Pogodin A.I., Filep M.J., Malakhovska T.O. *et al.* Microstructural, mechanical and electrical properties of superionic $Ag_{6+x}(P_{1-x}Ge_x)S_5I$ ceramic materials. *J. Phys. Chem. Solids*. 2022. **171**. P.111042. https://doi.org/10.1016/j.jpcs.2022.111042.
15. Elalfy D.A., Gouda E., Kotb M.F. *et al.* Comprehensive review of energy storage systems technologies, objectives, challenges, and future trends. *Energy Strategy Rev*. 2024. **54**. P. 101482. https://doi.org/10.1016/j. esr.2024.101482.
16. Pogodin A., Filep M., Malakhovska T. *et al.* Recrystallization and heterovalent substitution effects on mechanical and electrical parameters of $Ag_{6+x}(P_{1-x}Ge_x)S_5I$-based ceramics. *J. Eur. Ceram.*

Soc. 2023. **44**, No 6. P. 4097–4110. https://doi.org/10.1016/j.jeurceramsoc.2023.12.093.
17. Jiang S.P. Solid-state electrochemistry and solid oxide fuel cells: status and future prospects. *Electrochem. Energy Rev*. 2022. **5**. P. 21. https://doi.org/10.1007/s41918-022-00160-8.
18. Alsaç E.P., Nelson D.L., Yoon S.G. *et al.* Characterizing electrode materials and interfaces in solid-state batteries. *Chem. Rev.* 2025. **125**. P. 2009–2119. https://doi.org/10.1021/acs.chemrev.4c00584.
19. Alkhalidi A., Khawaja M.K., Ismail S.M. Solid-state batteries, their future in the energy storage and electric vehicles market. *Science Talks.* 2024. **11.** P. 100382. https://doi.org/10.1016/j.sctalk.2024.100382.
20. Pogodin A.I., Filep M.J., Malakhovska T.O. Preparation and properties of ceramic materials in the Ag_6PS_5I–Ag_7GeS_5I system. *Sci. Bull. Uzhhorod Univ. Ser. Chem.* 2023. **48**, No 2. P. 16–22. https://doi.org/10.24144/2414-0260.2022.2.16-22.
21. Jindal S., Singh S., Saini G.S.S., Tripathi S.K. Optimization of thermoelectric power factor of (013)-oriented Ag_2Se films via thermal annealing. *Mater. Res. Bull*. 2021. 145. P. 111525. https://doi.org/10.1016/j.materresbull.2021.111525.
22. Cao T., Shi X.L., Hu B. *et al.* Advancing Ag_2Se thin-film thermoelectrics via selenization-driven anisotropy control. *Nat. Commun*. 2025. **16**. P. 1555. https://doi.org/10.1038/s41467-025-56671-7.
23. Bilanych V.S., Slyvka A.A., Vorobiov S.I. *et al.* Charge-discharge processes in solid electrolyte heterostructures $Ag_{7-x}(Ge_{1-x}P_x)S_5I$ for electrochemical energy devices. *SPQEO.* 2026. **29**. P. 066–079. https://doi.org/10.15407/spqeo29.01.066.
24. Bard A.J., Faulkner L.R., White H.S. *Electrochemical Methods: Fundamentals and Applications* (3rd ed.). John Wiley & Sons, 2022.
25. Bilanych V.S., Skubenych K.V., Babilya M.I. *et al.* The effect of isovalent cation substitution on mechanical properties of$(Cu_xAg_{1-x})_7SiS_5I$ superionic mixed single crystals. *Ukr. J. Phys.* 2020. **65**, No 5. P. 453–457. https://doi.org/10.15407/ujpe65.5.453.
26. Bilanych V.V., Csach K., Flachbart K. *et al.* Investigation of the processes of softening and crystallization of glassy selenium by dynamic mechanical analysis method. *Sci. Herald Uzhhorod Univ. Ser. Phys*. 2018. **44**. P. 44–51. https://doi.org/10.24144/2415-8038.2018.44.44-50.
27. Wang L., Li J., Lu G. *et al.* Fundamentals of electrolytes for solid-state batteries: challenges and perspectives. *Front. Mater*. 2020. **7**. P. 111. https://doi. org/10.3389/fmats. 2020.00111.
28. Nie K., Hong Y., Qiu J. *et al.* Interfaces between cathode and electrolyte in solid state batteries: Challenges and perspectives. *Front. Chem.* 2018. **6**. P. 1–19. https://doi.org/10.3389/fchem.2018.00616.
29. Zhang S., Li Y., Bannenberg L.J. *et al.* The lasting impact of formation cycling on the Li-ion kinetics. *Sci. Adv.* 2024. **10**, No 3. P. 8889. https://doi.org/10.1126/sciadv.adj8889.
30. Fong K.D., Self J., Diederichsen K.M. *et al.* Ion transport and the transference number. *ACS Cent. Sci.* 2019. **5**, No 7. P. 1250–1260. https://doi.org/10.1021/acscentsci.9b00406.

Authors and CV

Vitaliy S. Bilanych, Assoc. Prof., CSc., Head of the Department of Applied Physics and Quantum Electronics, Uzhhorod National University. Authored over 90 publications and 4 patents. Areas of professional interest: study of nanostructuring and charge redistribution in chalcogenide films under electron and laser irradiation; charge-discharge processes and ion transport in solid-state cells based on superionic and chalcogenide materials; internal friction and relaxation in chalcogenide glasses; development of gas sensors using nanostructured oxides (SnO_2, In_2O_3) with Au/Pt nanoparticles. https://orcid.org/0000-0003-4293-5675

Anatoliy A. Slyvka, PhD student, Department of Applied Physics and Quantum Electronics, Uzhhorod National University. He is the author of 2 publications. The area of his scientific interests includes electron-photon emission from the surfaces of alkali halide crystals modified with metal nanoparticles and ion transport processes in superionic conductors with argyrodite-type structure. E-mail: anatolii.slyvka@uzhnu.edu.ua, https://orcid.org/0000-0002-9173-731X

Serhii I. Vorobiov, defended his PhD in Physics and Mathematics in 2015 at the Sumy State University, Ukraine. Postdoctoral researcher at the Institute of Physics, Faculty of Science, P.J. Safarik University, Slovakia. He is the author of 78 publications indexed in Scopus and Web of Science databases and 1 patent. The area of his scientific interests includes nanofabrication and thin film technology, and magnetic and magnetoresistance properties of nano and mesoscopic systems. E-mail: serhii.vorobiov@upjs.sk, https://orcid.org/0000-0002-5884-3292

Artem I. Pogodin, PhD in Inorganic Chemistry (2016), Senior Researcher at the Uzhhorod National University. Authored over 100 articles and 100 patents. The area of his scientific interests includes solid state chemistry, crystal growth, and materials science. E-mail: artempogodin88@gmail.com, https://orcid.org/0000-0002-2430-3220

Ihor M. Mohylyuk, received a M.Sc degree in applied physics and nanomaterials at the Uzhhorod National University, currently he is an Engineer of the Department of Applied Physics and Quantum Electronics at the same university. Research interests: gas-sensitive materials based on tin dioxide, superionic conductors.
E-mail:ihormohyliyk@gmail.com,
https://orcid.org/0009-0009-3871-0001

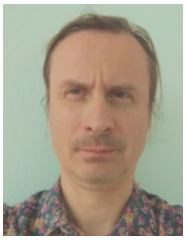

Vladimir Komanicky, defended his PhD thesis in Chemistry in 2003 at the University of California. Leading Scientist in the Electrocatalysis and Nanotechnology group at the Institute of Physics of the P.J. Safarik University in Kosice. Author of 141 publications, 2 patents and 2 textbooks. The area of his scientific interests includes nanotechnology, electrocatalysis, semiconductor physics, magnetism and superconductivity.
E-mail: vladimir.komanicky@upjs.sk,
https://orcid.org/0000-0001-8649-1987

Tetyana O. Malakhovska, PhD in Inorganic Chemistry (2010), Senior Researcher at the Uzhhorod National University. She is the author of more 70 articles and 10 patents. The area of her scientific interests includes solid state chemistry and materials science.
E-mail: t.malakhovska@gmail.com,
https://orcid.org/0000-0001-7309-4894

Authors' contributions

Bilanych V.S.: conceptualization, methodology, validation, supervision, writing – original draft.
Slyvka A.A.: investigation, validation, data curation.
Vorobiov S.I.: methodology, supervision, validation, investigation.
Pogodin A.I.: methodology, supervision, resources.
Malakhovska T.O.: methodology, formal analysis, data analysis, validation.
Mohylyuk I.M.: investigation, formal analysis.
Komanicky V.: conceptualization, validation, formal analysis, methodology, writing – review & editing.

Температурно-залежне накопичення заряду та вольт-амперні характеристики суперіонних гетероструктур $Ag_{7-x}(P_xGe_{1-x})S_5I$ для твердотільних енергетичних пристроїв

В.С. Біланич, А.А. Сливка, С.І. Воробйов, А.І. Погодін, Т.О. Малаховська, І.М. Могилюк, V. Komanicky

Анотація. У роботі досліджено температурно-залежні процеси накопичення та релаксації заряду, а також вольт-амперні характеристики гетероструктур $Ag|Ag_{7-x}(P_xGe_{1-x})S_5I|Se$ з різним співвідношенням Ge/P. Залежності струму $I(t)$ вивчали в потенціостатичному режимі (0.4 В, 600 с) з подальшою розрядкою (0 В, 600 с) при 20 °С та 60 °С. Показано, що релаксація описується двохекспоненціальною моделлю з часами τ_1 і τ_2, які відповідають швидким міжфазним та повільним дифузійним процесам. Установлено, що зі зростанням температури часи релаксації зменшуються внаслідок активації перенесення іонів Ag^+ та розм'якшення селену. Арреніус-аналіз показав відмінність енергій активації для швидких (~ 0.1…0.3 еВ) і повільних (~ 0.05…0.15 еВ) процесів. Вольт-амперні характеристики мають нелінійний і асиметричний характер з максимумами струму, пов'язаними з міжфазною поляризацією та утворенням Ag_2Se. Мінімальні часи релаксації спостерігаються для складу $Ag_{6.5}P_{0.5}Ge_{0.5}S_5I$.

Ключові слова: суперіонні провідники, аргіродитна структура, $Ag_{7-x}(P_xGe_{1-x})S_5I$, гетероструктури твердого електроліту, процеси заряджання-розряджання, міжфазна поляризація, твердотільні електрохімічні пристрої.